



## Connectomic markers of symptom severity in sport-related concussion: Whole-brain analysis of resting-state fMRI

Nathan W. Churchill<sup>a,\*</sup>, Michael G. Hutchison<sup>a,b</sup>, Simon J. Graham<sup>c,d</sup>, Tom A. Schweizer<sup>a,e,f</sup>

<sup>a</sup> Keenan Research Centre of the Li Ka Shing Knowledge Institute at St. Michael's Hospital, Neuroscience Research Program, St. Michael's Hospital, Toronto, ON, Canada

<sup>b</sup> Faculty of Kinesiology and Physical Education, University of Toronto, Canada

<sup>c</sup> Department of Medical Biophysics, University of Toronto, Toronto, ON, Canada

<sup>d</sup> Physical Sciences Platform, Sunnybrook Research Institute, Sunnybrook Health Sciences Centre, Toronto, ON, Canada

<sup>e</sup> Faculty of Medicine (Neurosurgery), University of Toronto, Toronto, ON, Canada

<sup>f</sup> The Institute of Biomaterials & Biomedical Engineering (IBBME) at the University of Toronto, Toronto, ON, Canada

### ARTICLE INFO

#### Keywords:

fMRI  
Functional connectivity  
Concussion  
Brain injury  
Symptoms

### ABSTRACT

Concussion is associated with significant adverse effects within the first week post-injury, including physical complaints and altered cognition, sleep and mood. It is currently unknown whether these subjective disturbances have reliable functional brain correlates. Resting-state functional magnetic resonance imaging (rs-fMRI) has been used to measure functional connectivity of individuals after traumatic brain injury, but less is known about the relationship between functional connectivity and symptom assessments after a sport concussion. In this study, rs-fMRI was used to evaluate whole-brain functional connectivity for seventy (70) university-level athletes, including 35 with acute concussion and 35 healthy matched controls. Univariate analyses showed that greater symptom severity was mainly associated with lower pairwise connectivity in frontal, temporal and insular regions, along with higher connectivity in a sparser set of cerebellar regions. A novel multivariate approach also extracted two components that showed reliable covariation with symptom severity: (1) a network of frontal, temporal and insular regions where connectivity was negatively correlated with symptom severity (replicating the univariate findings); and (2) a network with anti-correlated elements of the default-mode network and sensorimotor system, where connectivity was positively correlated with symptom severity. These findings support the presence of connectomic signatures of symptom complaints following a sport-related concussion, including both increased and decreased functional connectivity within distinct functional brain networks.

### 1. Introduction

Concussion is a form of mild traumatic brain injury (mTBI) which is associated with transient behavioural disturbances, typically in the absence of structural abnormalities for standard clinical neuroimaging (McCrorry et al., 2013; Yuh et al., 2014). Individuals with concussion may present with a range of signs and symptoms, including somatic complaints, impaired cognition and disturbances in mood and sleep (Guskiewicz et al., 2001; McCrea et al., 2003). The clinical assessment of sport-related concussion has been standardized with the development of the Sport Concussion Assessment Tool (SCAT), which has shown diagnostic utility for acute concussions (Guskiewicz et al., 2013; McCrorry et al., 2013; Echemendia et al., 2017). The SCAT has evolved over time, with the most recent versions, SCAT3 (Guskiewicz et al., 2013) and SCAT5 (Echemendia et al., 2017), combining previously separate assessments of symptoms, cognitive status, gross neurological

functioning and balance. Symptom evaluation is an integral element of the clinical assessment and assists clinicians in identifying the type and severity of functional disturbances. Furthermore, the utility of symptom evaluation has been consistently demonstrated, as greater initial symptom burden following concussion is associated with worse outcomes (Iverson et al., 2017; Makdissi et al., 2010, 2013; Putukian et al., 2015). Despite the critical role of symptom assessments in informing clinical management and determining safe return-to-play in sport and recreation, it is presently unknown whether these subjective measures are associated with reliable, objective measures of brain physiology. To better understand the etiology of behavioural disturbances after a sport-related concussion, it is important to examine the link between brain function at early injury and symptom endorsement.

Functional magnetic resonance imaging (fMRI) is a powerful tool for investigating altered brain function in concussed athletes, by measuring fluctuations in blood-oxygenation that are associated with neural

\* Corresponding author at: 209 Victoria Street, Toronto, ON M5B 1M8, Canada.  
E-mail address: [ChurchillN@smh.ca](mailto:ChurchillN@smh.ca) (N.W. Churchill).

activity. Task-based fMRI studies have typically reported increased activity in brain regions implicated in working memory tasks for athletes with concussion, compared to uninjured controls (Slobounov et al., 2012). Resting-state fMRI (rs-fMRI) has also been used to compute functional connectivity, which provides a measure of functional integration between brain regions (Van Den Heuvel and Pol, 2010). Prior rs-fMRI studies have reported significantly altered functional connectivity during the first week post-injury, when most athletes are still symptomatic (Churchill et al., 2017; Zhu et al., 2015) and also during the sub-acute phase from one week to one month post-injury, when most athletes are asymptomatic at rest (Johnson et al., 2012; Zhang et al., 2010; Zhu et al., 2015). Collectively, these studies have identified significant alterations in brain function within the first month following a sport-related concussion.

However, less is known about the relationship between resting brain function and the severity of post-concussion symptoms in athletes. Outside of the sport domain, rs-fMRI studies of mTBI have focused mainly on dysfunction of the default mode network (DMN), which has been reported to be a sensitive biomarker for disease and neurological insult (Garrity et al., 2007; Greicius et al., 2004). Mayer and colleagues scanned mTBI patients within 3 weeks post-injury (Mayer et al., 2011), showing that reduced DMN connectivity and increased inferior parietal connectivity were associated with more severe cognitive symptoms. Similarly, (Zhou et al., 2012) found that reduced DMN connectivity was associated with greater severity of endorsed symptoms (e.g., anxiety, depression and fatigue), for patients imaged an average of 3 weeks post-injury. More recently, (Messé et al., 2013) used rs-fMRI to study mTBI patients with persistent post-concussion syndrome, by parcellating the brain into 82 cortical and subcortical domains using an anatomical atlas and assessing inter-regional connectivity. They found that elevated symptoms were mainly correlated with reduced thalamic connectivity within 1–3 weeks post-injury and reduced frontal connectivity at 6 months post-injury.

The present rs-fMRI study extends these analyses to sport-related concussion, by examining a sample of university athletes with acute concussion and a sample of individually-matched healthy controls. We tested for associations between functional connectivity and SCAT3 symptom endorsements for concussed athletes within the first week post-injury, and compared these values to uninjured controls. The analyses were conducted using whole-brain techniques to avoid making a priori assumptions about the brain regions that show greatest association with symptom severity. Two approaches were adopted: first, a univariate analysis which tested for significant correlations between symptom severity and connectivity strength, for every pair of grey matter voxels in the brain; and second, a novel multivariate approach, which identified distributed functional brain networks that have maximum covariance with symptom severity. The multivariate approach was also used to compare functional network expression of athletes with concussion relative to the uninjured control group.

## 2. Materials and methods

### 2.1. Study participants

A sample of seventy (70) athletes were recruited from university level sport teams (volleyball, hockey, soccer, football, rugby, basketball and lacrosse) from a single institution, through the Sport Medicine Clinic. This included thirty-five (35) athletes with acute concussion and 35 matched control athletes. The concussed athletes (19/35 female; mean  $\pm$  SD age  $20.3 \pm 2.2$  years; a median of 1 concussion prior to the current injury, range 0 to 4) were recruited following a diagnosis of acute concussion by the referring physician, and imaged a median of 5 days post-injury (range of 1 to 7 days). The diagnosis was made by a staff physician, in accordance with Concussion in Sport Group guidelines (McCroory et al., 2013). Each athlete with concussion was matched to a control that had no documented concussions in the 6 months prior

to scanning. Controls (19/35 female, mean age  $20.3 \pm 1.7$  years, average history of 1 prior concussion, range 0 to 3) were individually matched to concussed athletes based on sex and prior number of concussions, as multiple concussions are associated with greater long-term consequences (McCroory et al., 2013) and altered brain function (Johnson et al., 2012). Matching was also performed with respect to age (mean difference:  $0.0 \pm 1.2$  years;  $p = 0.94$ , paired Wilcoxon test) to control for developmental differences.

Pre-season baseline symptoms were assessed for all participants as part of standard clinical protocol, using the SCAT3 (Guskiewicz et al., 2013), along with cognition, based on standardized assessment of concussion (SAC) scores (McCrea et al., 1997) and balance, based on modified Balance Error Scoring System (M-BESS) scores (Guskiewicz et al., 2013). The SCAT3 scores (symptoms, SAC and M-BESS) were also collected from athletes with acute concussion at the time of injury. This study was carried out in accordance with the recommendations of the Canadian Tri-Council Policy Statement 2 (TCPS2) and with approval of the research ethics boards of the University of Toronto and St. Michael's Hospital, with written informed consent from all subjects. All subjects gave written informed consent in accordance with the Declaration of Helsinki.

### 2.2. Magnetic resonance imaging

Athletes were imaged at St. Michael's Hospital using a research-dedicated MRI system operating at 3 Tesla (Magnetom Skyra, Siemens, Erlangen, Germany) with the standard 20-channel head receiver coil. Structural imaging included three-dimensional (3D) T1-weighted Magnetization Prepared Rapid Acquisition Gradient Echo (MPRAGE: inversion time (TI)/echo time (TE)/repetition time (TR) = 1090/3.55/2300 ms, flip angle (FA) =  $8^\circ$ , 192 sagittal slices with field of view (FOV) =  $240 \times 240$  mm,  $256 \times 256$  pixel matrix, 0.9 mm slice thickness,  $0.9 \times 0.9$  mm in-plane resolution, with bandwidth (BW) = 200 Hertz per pixel (Hz/px), fluid attenuated inversion recovery imaging (FLAIR: TI/TE/TR = 1800/387/5000 ms, 160 sagittal slices with FOV =  $230 \times 230$  mm,  $512 \times 512$  matrix, 0.9 mm slice thickness,  $0.4 \times 0.4$  mm in-plane resolution, BW = 751 Hz/px) and susceptibility-weighted imaging (SWI: TE/TR = 20/28 ms, FA =  $15^\circ$ , 112 axial slices with FOV =  $193 \times 220$  mm,  $336 \times 384$  matrix, 1.2 mm slice thickness,  $0.6 \times 0.6$  mm in-plane resolution, BW = 120 Hz/px). Structural images were reviewed in a 2-step procedure, consisting of initial inspection by an MRI technologist during the imaging session and later review by a neuroradiologist with clinical reporting, if any abnormalities were identified. Statistical testing was also performed by obtaining mean, variance and skew of voxel signal intensity distributions for masked MPRAGE, FLAIR and SWI images, generating a Z-score for each imaging sequence per athlete relative to the control distribution and identifying statistically significant outliers at  $p < 0.05$ . No abnormalities (white matter hyper-intensities, contusions, micro-hemorrhage, or statistical outliers) were found for the concussed athletes and controls in this study.

Resting-state fMRI was acquired via multi-slice T2\*-weighted echo planar imaging (EPI: TE/TR = 30/2000 ms, FA =  $70^\circ$ , 32 oblique-axial slices acquired interleaved ascending, with FOV =  $200 \times 200$  mm,  $64 \times 64$  matrix, 4.0 mm slice thickness with 0.5 mm gap,  $3.125 \times 3.125$  mm in-plane resolution, BW = 2298 Hz/px), producing a time-series of 195 images at each slice location. During acquisition, athletes were instructed to lie still with their eyes closed and to not focus on anything in particular. Processing and analysis were performed using the Analysis of Functional Neuroimages (AFNI) package ([afni.nimh.nih.gov](http://afni.nimh.nih.gov)) and customized algorithms developed in the laboratory. After discarding the first 4 volumes to allow scans to reach equilibrium, this included rigid-body motion correction (AFNI *3dvolreg*), removal of outlier scan volumes using the SPIKECOR algorithm ([nitrc.org/projects/spikecor](http://nitrc.org/projects/spikecor)), slice-timing correction (AFNI *3dTshift*), spatial smoothing with a 6 mm Full Width at Half Maximum (FWHM) isotropic

3D Gaussian kernel (AFNI *3dmerge*) and regression of motion parameters and linear-quadratic trends as nuisance covariates. For motion parameter regression, Principal Component Analysis was performed on the six rigid-body movement parameters, and the first two principal components were used as nuisance regressors. To control for physiological noise, the data-driven PHYCAA+ algorithm ([nitrc.org/projects/phycaa\\_plus](http://nitrc.org/projects/phycaa_plus)) was used to spatially down-weight areas with non-neural signal, followed by regression of white matter signal. The white matter regression was performed after spatial normalization and the generation of probabilistic tissue maps (see paragraph below for details), by regressing out the mean time-series computed over all white matter voxels ( $p > 0.95$ ).

To perform group-level connectivity analyses, the fMRI data were co-registered to a common anatomical template using the FMRIB Software Library (FSL) package (<https://fsl.fmrib.ox.ac.uk>). The FSL *flirt* algorithm was used to compute the rigid-body transform of the mean fMRI volume for each athlete to their T1-weighted anatomical image, along with the 12-parameter affine transformation of the T1 image for each athlete to the MNI152 template. The transformation matrices were then concatenated and the net transform applied to the fMRI data, which was resampled to  $4 \times 4 \times 4$  mm resolution to ensure computational tractability for the univariate analyses. To ensure that only grey matter brain regions were analyzed, voxels were retained that intersected with both the MNI152 brain mask and a grey matter mask. The latter was obtained by using the FSL *fast* algorithm (<https://fsl.fmrib.ox.ac.uk/fsl/fslwiki/FAST>) to segment subject T1 images into grey matter (GM), white matter (WM) and cerebrospinal fluid (CSF) maps. They were then transformed into MNI152 template space and resampled to  $4 \times 4 \times 4$  mm resolution before averaging across subjects. A mask was chosen to include only regions where  $p(\text{GM}) > p(\text{WM}) + p(\text{CSF})$ , before eroding the resulting mask using a disk element of diameter 3 voxels. Remaining voxels that overlapped with ventricles on the MNI152 template image were also removed manually. This procedure resulted in 18,401 voxels in the brain of each athlete that were used in subsequent analyses.

### 2.3. Clinical and demographic data

Analyses of SCAT3 symptoms focused on symptom severity, which was obtained by summing across a 22-item symptom scale, each with a 7-point Likert scale rating (Guskiewicz et al., 2013). Non-parametric paired Wilcoxon tests were used to test whether symptom severity scores and number of symptoms were elevated at acute concussion, relative to baseline scores and matched controls. A second set of analyses examined whether symptom severity scores at acute injury were correlated with demographic factors that included age, sex and number of prior concussions. Correlations were estimated using non-parametric Spearman correlations, along with bootstrapped 95% confidence intervals (CIs) based on 1000 resampling iterations. Multiple comparison correction was conducted at a False Discovery Rate (FDR) of 0.05.

### 2.4. Neuroimaging analysis and symptoms

#### 2.4.1. Univariate analysis

An initial set of univariate analyses were conducted to identify pairs of voxels where connectivity strength was reliably correlated with symptom severity scores. For each pair of voxels  $(i, j)$ , functional connectivity  $\rho(i, j)_s$  was calculated per athlete ( $s = 1 \dots 35$ ) based on the Pearson correlation coefficient. The correlation was then measured between connectivity strength values  $\rho(i, j)_s$  and symptom severity scores  $y_s$ . Significance was assessed in a non-parametric bootstrap resampling framework to minimize distributional assumptions. This was done by computing an empirical  $p$ -value based on the fraction of resamples overlapping zero, with post-hoc correction for multiple comparisons at an FDR of 0.05. For these analyses, the  $y_s$  values were rank-normalized across subjects to avoid bias caused by heavy distribution

tails (kurtosis: 4.48, deviating from normality at  $p = 0.025$ ). The results were then summarized as a pair of voxel-wise brain maps, which depict (1) the fraction of functional connections to other voxels that had a significant positive correlation with symptom scores; and (2) the fraction of connections that had a significant negative correlation with symptom scores. This was used to assess the relative sensitivity of individual brain regions to the effects of symptom severity.

#### 2.4.2. Multivariate analysis

A novel multivariate approach was used to identify functional networks (i.e., distributed sets of brain regions) where intra-network connectivity was most strongly associated with symptom severity scores. The model was built within the widely-used partial least squares (PLS) regression framework (Krishnan et al., 2011; Rosipal and Krämer, 2006). Given a vector of “input” variables  $\mathbf{x}_s$  and a “response” variable  $y_s$ , acquired for a set of subjects  $s = 1 \dots S$ , PLS estimates a latent vector  $\mathbf{a}$  of weightings on input data, which produces subject scores  $c_s = \mathbf{a}^T \mathbf{x}_s$  that have maximum covariance with  $y_s$ . This approach has been extended to higher-order input data (i.e., matrices and higher-order tensors) by (Bro, 1996), in an approach termed N-way partial least squares (NPLS). For a set of 2D input data matrices  $\mathbf{X}_s$ , NPLS identifies paired latent vectors  $\mathbf{a}, \mathbf{b}$ , where the subject scores  $c_s = \mathbf{a}^T \mathbf{X}_s \mathbf{b}$  have maximum covariance with response variable  $y_s$ . The NPLS approach was extended in the present work to analyze functional connectivity matrices in fMRI data, using a model subsequently referred to as symmetric N-way partial least squares (Sym-NPLS).

In the Sym-NPLS model, each subject has an fMRI data matrix  $\mathbf{X}_s$  consisting of  $(V \text{ voxels} \times T \text{ timepoints})$  and the input data are the set of  $(V \times V)$  whole-brain functional connectivity matrices, computed via pairwise Pearson correlation between voxel timeseries. For vectors  $(i, j)$  with zero mean and unit length,  $\text{corr}(i, j) = \mathbf{x}_{(i)} \cdot \mathbf{x}_{(j)}$ ; hence, if each voxel timeseries in  $\mathbf{X}_s$  has the temporal mean subtracted and is rescaled to unit length, then the  $(V \times V)$  correlation matrix for subject  $s$  is  $\mathbf{X}_s \mathbf{X}_s^T$ . A latent pattern of voxel weightings  $\mathbf{a}$  is then sought, which represents a functional brain network where connectivity has maximum covariance with the response variable  $y_s$ . Within-network connectivity for subject  $s$  is quantified by the bilinear projection of  $\mathbf{a}$  onto their whole-brain correlation matrix:

$$c_s = \mathbf{a}^T (\mathbf{X}_s \mathbf{X}_s^T) \mathbf{a}, \quad (1)$$

which produces a positive, scalar “subject score”  $c_s$ , reflecting total network connectivity for this subject. It is possible to solve for  $\mathbf{a}$  by maximizing the expression  $\text{cov}(c, y) = \sum_s (c_s - \bar{c})(y_s - \bar{y})$ . Substituting Eq. (1) into this expression, this becomes:

$$\text{cov}(c, y) = \sum_s \left( \mathbf{a}^T (\mathbf{X}_s \mathbf{X}_s^T) \mathbf{a} - \left[ \frac{1}{S} \sum_{s'} \mathbf{a}^T (\mathbf{X}_{s'} \mathbf{X}_{s'}^T) \mathbf{a} \right] \right) \left( y_s - \frac{1}{S} \sum_{s'} y_{s'} \right), \quad (2)$$

Expanding and centering the response variable of Eq. (2) (i.e., setting  $\bar{y} = 0$ ) reduces to:

$$\text{cov}(c, y) = \mathbf{a}^T \left[ \sum_s (\mathbf{X}_s \mathbf{X}_s^T) \right] \mathbf{a}, \quad (3)$$

This quadratic-form expression is maximized for  $\mathbf{a}$  when it is an eigenvector of  $[\sum_s (\mathbf{X}_s \mathbf{X}_s^T)]_s$ . This matrix has a total rank of  $\sum_s T_s^*$ , where  $T_s^* \leq T$  denotes the rank of individual subject data matrices  $\mathbf{X}_s$ . Therefore, an eigen-decomposition of this matrix generates up to  $k = 1 \dots K$  ( $K \leq \sum_s T_s^*$ ) orthonormal components, or spatial weighting vectors  $\mathbf{a}_k$ . These vectors are used to generate the subject scores  $c_{ks}$  that have maximal covariance with symptom severity scores  $y_s$ .

To confirm that Sym-NPLS extracts functional brain patterns of maximum covariance with a response variable of interest, this model was applied to synthetic data in Supplementary Text S1, showing robust performance. Moreover, because Sym-NPLS analyses were conducted on  $(V \times V)$  whole-brain connectivity matrices, an initial data compression step was essential for computational tractability. This was

performed using sequential Principal Component Analysis (PCA) decompositions to reduce the rank of input data, described in further detail in Supplementary Text S2, where a 97.42% reduction in dimensionality of the input data was obtained, without altering the extracted spatial patterns.

**2.4.2.1. Statistical inference.** Statistical testing of the spatial weighting vectors  $\mathbf{a}_k$  was conducted in a non-parametric bootstrap resampling framework. Subjects were resampled with replacement to obtain bootstrapped estimates  $\{\mathbf{a}_k^{(b)}\}_{k=1}^K$  for the  $b$ th resampling iteration. Because components of the eigen-decomposition may be arbitrarily reordered between bootstrap samples, each set of  $\{\mathbf{a}_k^{(b)}\}_{k=1}^K$  were matched to a fixed  $\{\mathbf{a}_k^{(0)}\}_{k=1}^K$  estimated from the whole dataset, using restricted Procrustes matching to flip the sign and permute the order of components. As this procedure has no closed-form solution, a “greedy search” was conducted by successively matching the component pair  $\mathbf{a}_k^{(b)}$  and  $\mathbf{a}_k^{(0)}$  of highest correlation. The effect sizes for individual voxel saliences were then computed as bootstrap ratios (i.e., the bootstrapped mean/standard error) with significance estimated by calculating an empirical  $p$ -value based on the normally-distributed bootstrap ratio values. Adjustment for multiple comparisons was performed at an FDR of 0.05. Confidence intervals of subject scores  $c_s$  were also obtained by calculating the scores at each bootstrap sample,  $c_{ks}^{(b)} = \mathbf{a}_k^{(b)T}(\mathbf{X}_s\mathbf{X}_s^T)\mathbf{a}_k^{(b)}$  and generating normal standard error bounds on the  $c_{ks}^{(b)}$  for each subject.

The Sym-NPLS model was also used to perform statistical comparison of concussed athletes relative to the sample of uninjured, matched controls. For each control, the bilinear projection was performed of their functional connectivity matrix onto  $\mathbf{a}_k$ , generating the corresponding subject scores  $c_{ks}^{(ctrl)}$ . This set of scores was then used to fit a normal distribution, for the construction of 90% and 95% CIs. This allowed the testing of whether individual concussed athlete scores  $c_{ks}$  were significantly distinguishable from the set of  $c_{ks}^{(ctrl)}$  produced by healthy, uninjured athletes.

### 3. Results

#### 3.1. Clinical and demographic data

Table 1 summarizes participant demographics and clinical presentation. Prior to injury, symptom severity scores were comparable between concussed athletes and controls (mean difference  $\pm$  standard error:  $0.8 \pm 1.6$ ;  $p = 0.38$ , paired Wilcoxon test). At acute injury, concussed athletes had significantly higher symptom scores relative to their baseline (mean change:  $17.0 \pm 3.9$ ) and relative to the matched controls (mean difference:  $16.9 \pm 4.2$ ), both with  $p < 0.001$ , significant at an FDR of 0.05. At acute injury, SAC and M-BESS subscales

**Table 1**  
Athlete demographics. Age is reported as mean  $\pm$  SD, all other distributions are reported as median [min, max]. Symptom scores with \*\* denote significant difference at acute injury, relative to both within-subject baseline and controls.

	Control	Concussion	
		Baseline	Acute
Age (mean $\pm$ SD)	20.3 $\pm$ 1.7	20.3 $\pm$ 2.2	
Female	19/35	19/35	
Previous concussions	0 [0,3]	1 [0,4]	
Symptoms			
Severity	3 [0,29]	3 [0,24]	11 [0,90]**
Number of symptoms	2 [0,16]	3 [0,13]	8 [0,22]**
Cognition and balance			
Orientation	5 [4,5]	5 [4,5]	5 [4,5]
Immediate memory	15 [9,15]	15 [13,15]	15 [13,15]
Concentration	3 [1,5]	4 [2,5]	4 [2,5]
Delayed memory	4 [1,5]	5 [0,5]	4 [1,5]
M-BESS total errors	1 [0,10]	3 [0,12]	3 [0,12]

were not significantly different from baseline or matched controls ( $p > 0.23$ , all tests). In addition, the severity of acute symptoms was not significantly correlated with age (Spearman rho  $\rho = 0.05$ ,  $p = 0.76$ ), sex ( $\rho = 0.19$ ,  $p = 0.27$ ) or history of concussion ( $\rho = -0.07$ ,  $p = 0.70$ ). Acute symptom severity and the symptom change (acute – baseline) were also highly correlated ( $\rho = 0.89$ ,  $p < 0.001$ , significant at an FDR of 0.05).

#### 3.2. Neuroimaging and symptoms

For univariate analyses, 2.07% of all pairwise connections were significantly correlated with symptom severity scores at an FDR of 0.05. Fig. 1 displays a voxel-wise map of the percentage of connections showing significant correlations with symptom scores, thresholded to display the top 10% of most affected voxels. A spatially distributed set of brain regions showed decreased connectivity with greater symptom severity (Fig. 1A), with peaks seen in the bilateral parahippocampal gyri (slice 25), inferior orbitofrontal lobes (slices 25–30), along with the temporal lobes and posterior insula (slices 35–40). More dorsally, peaks were also seen in the posterior midcingulate (slice 60) and supplementary motor area (slices 65–70). Conversely, fewer regions showed increases in connectivity with greater symptom severity (Fig. 1B) with peaks predominantly in the cerebellum (slices 20–30), but also extending into the visual cortex (slices 35, 45), cuneus (slices 50–55) and superior frontal lobe (slice 70).

For multivariate analyses, bootstrap resampling produced two components ( $k = 1$  and 2) with significant voxel saliences after adjusting for multiple comparisons at an FDR of 0.05. Results for the first Sym-NPLS component are shown in Fig. 2. The spatial pattern  $\mathbf{a}_1$  is depicted in Fig. 2A, indicating an extensive pattern of significant brain regions. This pattern also shows strong associations with the univariate maps, exhibiting a Pearson correlation of 0.624 with the negative connectivity map (Fig. 1A) and a Pearson correlation of  $-0.496$  with the positive connectivity map (Fig. 1B). Regions with significant positive bootstrap ratios include the inferior orbitofrontal lobes (slices 25–30), superior and middle temporal lobes (slices 30–45), posterior insula (slices 35–45), inferior frontal lobes (slices 45–50), posterior midcingulate (slice 60), supplementary motor area (slices 65–70) and superior frontal regions (slices 65–75). In addition, negative bootstrap ratios are seen in the cerebellum (slices 20–30), indicating anti-correlations with positive brain regions. Fig. 2B plots concussed athlete subject scores  $c_{1s}$  against symptom severity scores, which has a negative correlation ( $-0.427$ , 95%CI:  $-0.659$ ,  $-0.312$ ;  $p = 0.010$ ) indicating that higher symptom severity is associated with reduced intra-network connectivity. The mean, as well as 90% and 95% CIs of the scores for healthy athlete controls are also shown for comparison, indicating that only a few athletes with low symptom scores were significantly different from controls. Fig. 2C plots representative subject connectivity maps for the top 10% of voxels in  $\mathbf{a}_1$  with the highest bootstrap ratio values. Confirming the interpretation of Fig. 2B, athletes with low symptom severity scores and significantly elevated  $c_{1s}$  scores relative to controls (denoted L1, L2 and L3) had high functional connectivity, compared to the athletes with high symptom scores and low  $c_{1s}$  scores (denoted H1, H2 and H3).

Results for the second Sym-NPLS component are depicted in Fig. 3. The spatial pattern  $\mathbf{a}_2$  is shown in Fig. 3A, with a much sparser set of significant brain regions observed in comparison to  $\mathbf{a}_1$ . The pattern  $\mathbf{a}_2$  shows little similarity with the univariate maps, with a Pearson correlation of 0.004 with the negative connectivity map (Fig. 1A) and 0.104 with the positive connectivity map (Fig. 1B). Brain regions with positive bootstrap values included the supramarginal gyri (slices 50–55), anterior midcingulate (slice 60), supplementary motor area (slices 65–70), left precentral gyrus (slice 65) and right superior frontal lobe (slice 70). These regions were anti-correlated with areas having negative bootstrap values, including medial orbitofrontal (slices 30–35), superior medial frontal (slices 50–55), along with anterior cingulate (slices



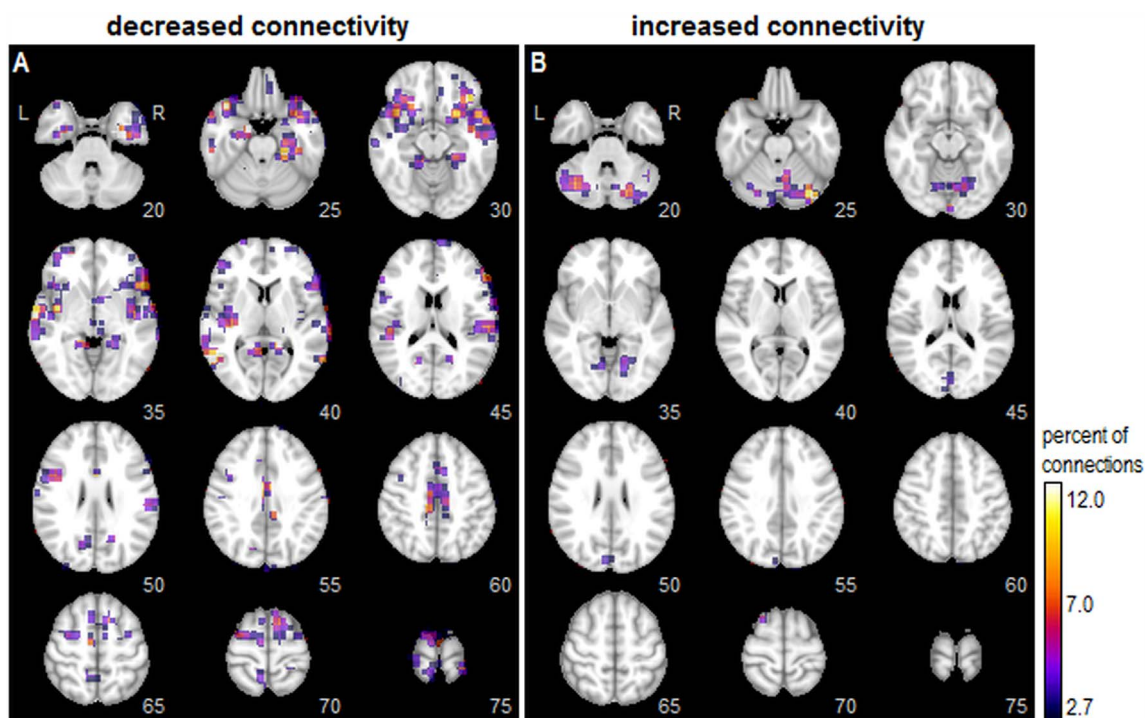


**Fig. 1.** Univariate whole-brain analysis of functional connectivity correlates with symptom severity. For each node (voxel), the color map indicates the percentage of all pairwise connections to other nodes in which connectivity strength is significantly correlated with symptom severity scores (bootstrapped  $p$ -values, at an FDR of 0.05). The brain maps separately show regions where greater symptom severity is correlated with (A) decreased connectivity and (B) increased connectivity. Maps are thresholded to show the top 10% of voxels with the greatest number of significant connections. (For interpretation of the references to color in this figure legend, the reader is referred to the web version of this article.)

35–40) and posterior cingulate cortex (slices 50–55). Fig. 3B plots concussed athlete subject scores  $c_{2s}$  against symptom severity scores, for which a positive correlation (0.580, 95%CI: 0.303, 0.677;  $p < 0.001$ ) indicates that greater symptom severity is associated with increased intra-network connectivity. The mean as well as 90% and 95% CIs of the scores for healthy athlete controls are again shown for comparison, indicating that for this component, individuals with high symptom scores were significantly distinct from controls. Fig. 3C plots representative athlete connectivity maps, shown for the top 10% of voxels in  $a_1$  with highest bootstrap ratio values. Athletes with low symptom severity scores (L1, L2 and L3) had positive functional connectivity between most regions, whereas those with higher symptom severity scores and significantly elevated  $c_{2s}$  scores relative to controls (H1, H2 and H3) had strong anti-correlations between positive and negative network nodes.

#### 4. Discussion

This study examined the relationship between symptom severity and resting brain function among recently concussed athletes. Functional connectivity was investigated for the whole brain, rather than among a set of predefined regions of interest, revealing significant associations with symptom severity distributed throughout the brain. This was evaluated using both univariate pairwise correlations and a novel multivariate approach, termed Sym-NPLS, which extracted functional networks that had maximal covariation with symptom scores. Both models were able to detect robust functional connectomic signatures of subjective symptom impairments during the sub-acute phase of sport concussion.

The univariate results showed generally lower pairwise functional connectivity, for athletes with concussion that had higher symptom severity scores. These findings are consistent with studies of non-sport mTBI that reported decreased functional connectivity for patients with greater symptom severity (Mayer et al., 2011; Messé et al., 2013; Zhou et al., 2012). The effects were most extensive in temporal and superior

frontal regions, which are critical to multiple aspects of cognition. The frontal lobes are involved in executive function (Badre, 2008) and the superior frontal gyri in particular are implicated in motor function, working memory and attention (Li et al., 2013). The temporal lobes are involved in language and auditory processing, but clinical studies have also linked regional atrophy to impairments in memory and cognition (Mummery et al., 2000; Pearlson, 1997; Shenton et al., 2001). Altered connectivity was also seen in the parahippocampal gyri, which play a key role in memory (Squire and Zola-Morgan, 1991) and, relevant to sports, spatial memory (Burgess et al., 2002). Dysfunction in these brain regions is important to consider, as impairments in cognition and memory are common symptoms of concussion (McCroory et al., 2013). Another affected area was the posterior midcingulate cortex, which plays a role in bodily orientation in space (Vogt, 2016). This is relevant to concussion, as issues of balance and dizziness are widely-reported post-concussion symptoms. The insula also showed altered functional connectivity and is involved in autonomic regulation (Critchley, 2005), along with physiological response to salient stimuli (Menon and Uddin, 2010). Increases in functional connectivity were mainly limited to the cerebellum, suggesting a distinct, potentially compensatory role for athletes with greater symptom impairment. This is supported by studies showing that the cerebellum is involved in domains beyond simple motor function, including memory, attention and executive function (Schweizer et al., 2007, 2008; Strick et al., 2009).

The multivariate Sym-NPLS model provided further insight into the relationship between functional connectivity and post-concussion symptoms, by extracting functional brain networks where within-network connectivity was associated with symptom severity scores. The first Sym-NPLS component was similar to the univariate map of affected brain areas. This indicates that the univariate effects of symptom severity may be largely attributable to decreased coherence within a single distributed functional network that included temporal, insular, frontal and midcingulate regions. The relationship between this network and clinical presentation after injury is supported by studies of head injury biomechanics, which have shown that frontotemporal brain

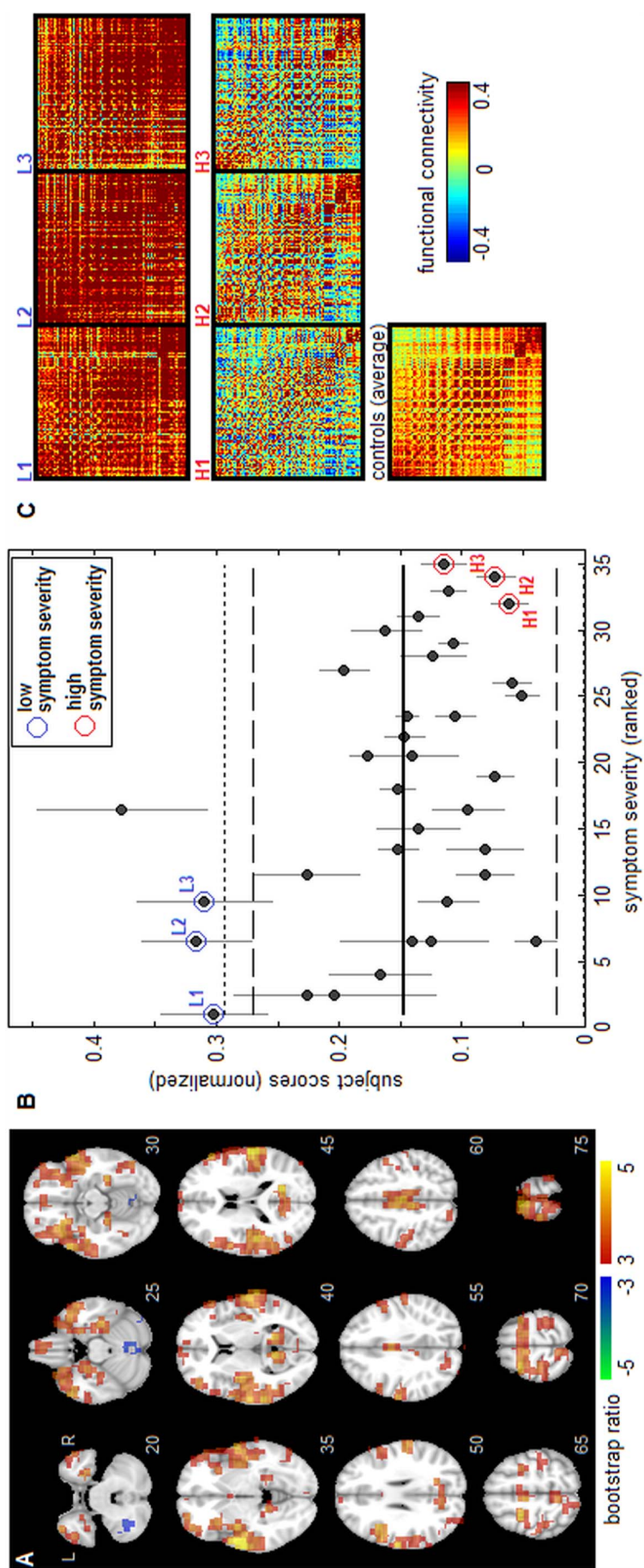


**Fig. 2.** The first component of multivariate whole-brain analysis of functional connectivity correlates with symptom severity. (A) Voxel salience map  $\alpha_1$ , with effect size reported as bootstrap ratios. (B) Concussed athlete “subject scores”, reflecting how strongly they express the functional pattern depicted in panel A, are plotted against ranked symptom severity scores. Horizontal lines show the mean (solid line), 90% CI (dashed lines) and 95% CI (dotted lines) of control athletes subject scores at baseline testing. (C) Functional connectivity plots for the top 10% of voxels with highest bootstrap ratios in panel A, for representative concussed athletes with low symptom scores (L1, L2, L3) and with high symptom scores (H1, H2, H3), along with the mean connectivity map averaged over all controls.

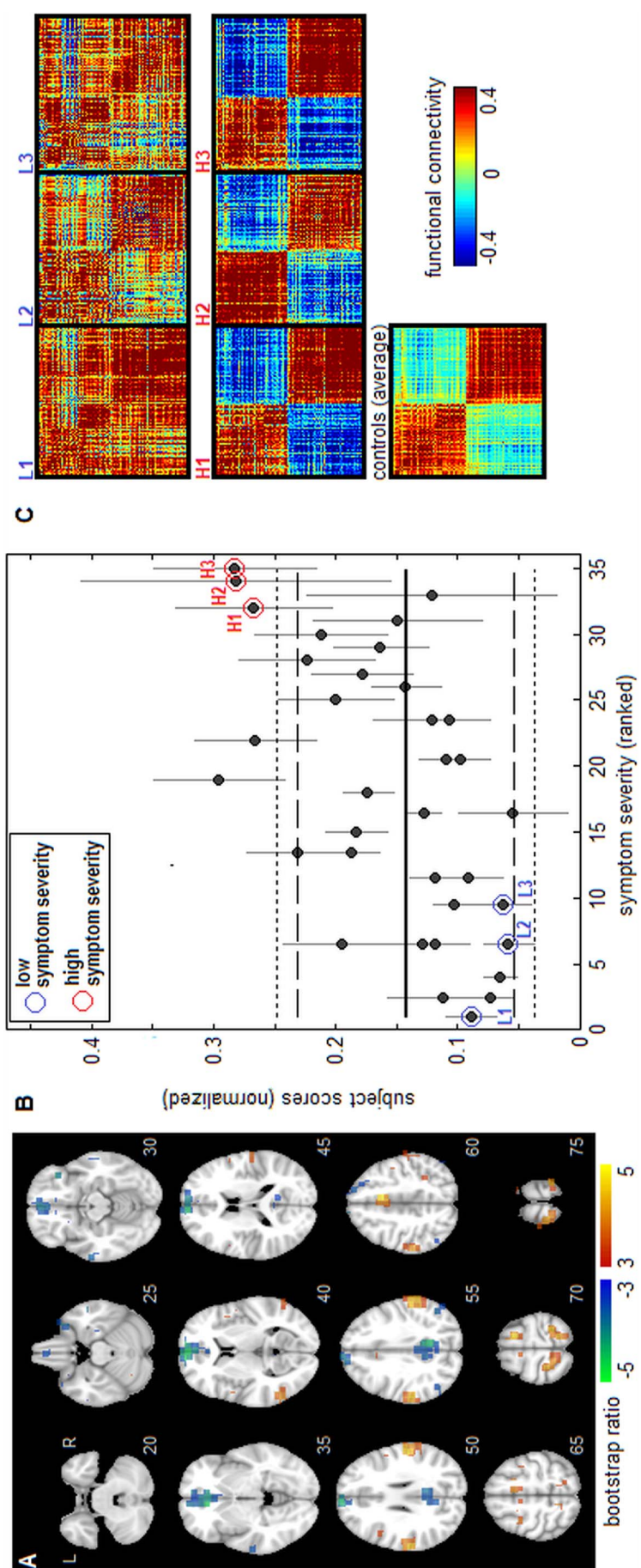


**Fig. 3.** The second component of multivariate whole-brain analysis of functional connectivity correlates with symptom severity. (A) Voxel salience map  $\alpha_2$  with effect size reported as bootstrap ratios. (B) Concussed athlete “subject scores”, reflecting how strongly they express the functional pattern depicted panel A (total network connectivity, including both positive and negative regions), are plotted against ranked symptom severity scores. Horizontal lines show the mean (solid line), 90% CI (dashed lines) and 95% CI (dotted lines) of control athletes subject scores at baseline testing. (C) Functional connectivity plots for the top 10% of voxels with highest bootstrap ratios in panel A, for representative concussed athletes with low symptom scores (L1, L2, L3) and with high symptom scores (H1, H2, H3), along with the mean connectivity map averaged over all controls.



regions are vulnerable to direct impact against bony ridges of the skull (Graham et al., 2002; Guskiewicz and Mihalik, 2006) and symptoms of dizziness are correlated with high levels of orbitofrontal and temporal strain during impact (Viano et al., 2005). Similarly, sub-cortical grey matter may be vulnerable to the delayed effects of strain propagating through the brain after a collision (Viano et al., 2005).

For the first Sym-NPLS component, a comparison of subject scores between athletes with concussion and matched controls also showed that only the athletes with lowest symptom scores had significantly different intra-network connectivity, relative to healthy controls. These results expand our understanding of the relationship between brain function and symptom severity, as connectivity values that exceed the “normal” range for this functional network are associated with a better initial clinical presentation. One interpretation of this finding is that elevated functional connectivity is an adaptive response following acute injury. This has been discussed in a review by (Hillary et al., 2015), which suggests that hyper-connectivity of the brain is a common outcome of mild neurological injury and may be an adaptive response to network disruption. However, in the absence of baseline neuroimaging, it is equally plausible that the athletes with lower symptom scores had elevated pre-injury functional connectivity, which then remained elevated after their injury. In this case, greater intrinsic connectivity between frontal, temporal and insular regions would serve as a protective role. The results of this study require further research with prospective scanning of athletes to determine whether they constitute a pre- or post-injury marker for acute symptom burden.

The second component identified by Sym-NPLS showed a sparser pattern of brain regions, which was spatially uncorrelated with univariate results. As shown in the connectivity plots of Fig. 3C, participants with higher symptoms have greater anti-correlation between positive and negative nodes of the functional network. Therefore, elevated connectivity cannot be considered a uniform marker of better clinical presentation following brain injury, as the relationship with symptoms depends on anatomical regions being investigated. These findings also highlight the advantage of a multivariate approach, as univariate analyses were unable to detect this more complex relationship between brain function and symptoms. For this component, symptom severity scores were related to connectivity strength between medial nodes of the DMN (posterior and ventral anterior cingulate) and other regions generally active during task engagement, including supramarginal gyri, supplementary motor area, midcingulate cortex, along with precentral and superior frontal gyri. Hence, anti-correlation of sensorimotor regions with the DMN may be a marker of elevated symptom severity. It has been previously shown that network anti-correlations with the DMN can be modulated by changes in physiological state, including caffeine consumption (Wong et al., 2012). The present results may reflect a more taxed mental state, as greater anti-correlation of task-positive networks with DMN has been related to task difficulty and the stability of behavioural performance (Kelly et al., 2008; Sala-Llonch et al., 2012); increased anti-correlation has also been observed in some mental disorders (Broyd et al., 2009). As with the first component, due to a lack of baseline imaging, it is not clear whether anti-correlation between these brain regions is a consequence of functional network disturbances after a concussion, or whether individuals with greater pre-injury network anti-correlation are more vulnerable to the effects of acute concussion. Nonetheless, compared to matched controls, this component showed that individuals with high symptoms had network connectivity that was significantly different from healthy individuals. Based on these findings, markers specifically distinguishing highly symptomatic athletes with concussion from controls maybe involve a set of reliable but spatially sparse brain regions.

Functional connectivity effects were greatest in brain regions that are consistent with typical post-concussion symptoms, e.g., cognition, memory and physical orientation. However, it is important to note that the SCAT3 findings were limited to self-reported symptoms. The participants in this study had no significant impairments in tests of

cognition (i.e., SAC) or balance (i.e., M-BESS), possibly because they are designed as brief screening tools and may be insensitive to subtle changes in cognition and visual-motor function. For the SAC, significant ceiling effects are widely reported (Echemendia et al., 2017), while the BESS has good specificity but low-to-moderate sensitivity (Giza et al., 2013). The present study was also limited to the modified version of BESS and the full protocol may have yielded different results. The sample of athletes with concussion in this study did not experience gross disturbances in brain function associated in cognition and balance, which is consistent with most of the athlete scores for functional brain networks that fell within “normal” bounds defined by uninjured controls (Figs. 2B, 3B). Additional tests pertaining to cognition (e.g., computerized neurocognitive testing), balance (e.g., postural sway), or oculomotor function, may provide better sensitivity and specificity when assessing patient outcome. At present, more detailed testing and follow-up is needed to definitively establish whether objective functional deficits underlie the identified relationships between brain function and symptoms.

This study showed reliable associations between symptom severity and functional connectivity, however, there are limitations which should be addressed in future research. This study had a cross-sectional design and it is therefore unknown how the brain function of concussed athletes compared to pre-injury brain function. Further research with prospective baseline scanning of athletes (see, e.g., (Bazarian et al., 2012)) is required to determine whether the findings of this study reflect functional disturbances caused by concussion, or differences in brain function that precede injury. Similarly, early symptom burden is related to prolonged recovery time (Makdissi et al., 2010, 2013; Putukian et al., 2015), however, future longitudinal studies are required to establish whether the observed functional markers of acute symptom severity are correlated with long-term clinical recovery. Finally, the present analyses focused on symptom assessments, which despite being a cornerstone of clinical management (Echemendia et al., 2017; Guskiewicz et al., 2013), are inherently subjective. While the present findings support a robust relationship between brain function and symptoms, future neuroimaging research may benefit from combining symptom reports with neurocognitive tests, along with assessments of psychological and environmental factors that may affect how athletes perceive and disclose symptoms after a concussion.

The multivariate analyses in this study were based on Sym-NPLS, which is an extension of partial least square (PLS) that is able to detect whole-brain functional networks associated with symptom scores. As a variant of PLS, it has similar model properties, including stability in the presence of high-dimensional input data. Although PCA-based dimensionality reduction was performed prior to analysis, this was done to reduce computational burden during resampling, as PLS-based models do not require regularization or parameter tuning to obtain reliable brain patterns associated with behaviour (Krishnan et al., 2011). However, Sym-NPLS maximizes covariance between brain function and behaviour, and will therefore tend to identify functional networks that account for both correlation with behaviour and variance within the rs-fMRI data (Rosipal and Krämer, 2006). If one is only interested in maximizing prediction of behaviour, an alternative cost function, such as least-squares regression, may be more appropriate. Nonetheless, to our knowledge, this is the first multivariate model to directly identify whole-brain connectivity patterns of greatest covariance with a behavioural outcome, in an efficient, computationally tractable manner.

This study has helped to extend our understanding of the relationship between initial symptom presentation and resting brain function following sport-related concussion. A combination of univariate and multivariate methods has shown that elevated frontotemporal connectivity is a marker of low symptom impairment following acute injury, while multivariate methods also revealed that anti-correlation between DMN and sensorimotor regions constitutes a specific marker of higher symptom severity. These results provide promising evidence that



reliable connectomic markers may be identified relating to the symptom burden after sport-related concussion.

## Acknowledgements

This work was supported by the Canadian Institutes of Health Research (CIHR) [grant number RN294001–367456]; the Canadian Institutes of Military and Veterans Health (CIMVHR) [grant number W7714-145967]; and pilot funding from Siemens Canada Ltd.

## Appendix A. Supplementary data

Supplementary data to this article can be found online at <https://doi.org/10.1016/j.nicl.2018.02.011>.

## References

- Badre, D., 2008. Cognitive control, hierarchy, and the rostro-caudal organization of the frontal lobes. *Trends Cogn. Sci.* 12, 193–200.
- Bazarian, J.J., Zhu, T., Blyth, B., Borrino, A., Zhong, J., 2012. Subject-specific changes in brain white matter on diffusion tensor imaging after sports-related concussion. *Magn. Reson. Imaging* 30, 171–180.
- Bro, R., 1996. Multiway calibration. Multilinear PLS. *J. Chemom.* 10.
- Broyd, S.J., Demanuele, C., Debener, S., Helps, S.K., James, C.J., Sonuga-Barke, E.J., 2009. Default-mode brain dysfunction in mental disorders: a systematic review. *Neurosci. Biobehav. Rev.* 33, 279–296.
- Burgess, N., Maguire, E.A., O'Keefe, J., 2002. The human hippocampus and spatial and episodic memory. *Neuron* 35, 625–641.
- Churchill, N.W., Hutchison, M.G., Richards, D., Leung, G., Graham, S.J., Schweizer, T.A., 2017. The first week after concussion: blood flow, brain function and white matter microstructure. *NeuroImage Clin.* 14, 480–489.
- Critchley, H.D., 2005. Neural mechanisms of autonomic, affective, and cognitive integration. *J. Comp. Neurol.* 493, 154–166.
- Echemendia, R.J., Broglio, S.P., Davis, G.A., Guskiewicz, K.M., Hayden, K.A., Leddy, J.J., Meehan, W.P., Putukian, M., Sullivan, S.J., Schneider, K.J., 2017. What tests and measures should be added to the SCAT3 and related tests to improve their reliability, sensitivity and/or specificity in sideline concussion diagnosis? A systematic review. *Br. J. Sports Med.* 51, 895–901.
- Garrity, A., Pearlson, G., McKiernan, K., Lloyd, D., Kiehl, K., Calhoun, V., 2007. Aberrant “default mode” functional connectivity in schizophrenia. *Am. J. Psychiatr.* 164, 450–457.
- Giza, C.C., Kutcher, J.S., Ashwal, S., Barth, J., Getchius, T.S., Gioia, G.A., Gronseth, G.S., Guskiewicz, K., Mandel, S., Manley, G., 2013. Summary of evidence-based guideline update: evaluation and management of concussion in sports Report of the Guideline Development Subcommittee of the American Academy of Neurology. *Neurology* 80, 2250–2257.
- Graham, D., Gennarelli, T., McIntosh, T., 2002. *Trauma. Greenfield's Neuropathology.* Oxford University Press, New York.
- Greicius, M., Srivastava, G., Reiss, A., Menon, V., 2004. Default-mode network activity distinguishes Alzheimer's disease from healthy aging: evidence from functional MRI. *PNAS* 101, 4637–4642.
- Guskiewicz, K.M., Mihalik, J.P., 2006. The biomechanics and pathomechanics of sport-related concussion. In: *Foundations of Sport-related Brain Injuries.* Springer, pp. 65–83.
- Guskiewicz, K.M., Ross, S., Marshall, S., 2001. Postural stability and neuropsychological deficits after concussion in collegiate athletes. *J. Athl. Train.* 36, 263.
- Guskiewicz, K., Register-Mihalik, J., McCrory, P., McCrea, M., Johnston, K., Makkidssi, M., Meeuwisse, W., 2013. Evidence-based approach to revising the SCAT2: introducing the SCAT3. *Br. J. Sports Med.* 47, 289–293.
- Hillary, F., Roman, C., Venkatesan, U., Rajtmajer, S., Bajo, R., Castellanos, N., 2015. Hyperconnectivity is a fundamental response to neurological disruption. *Neuropsychology* 29, 59.
- Iverson, G.L., Gardner, A.J., Terry, D.P., Ponsford, J.L., Sills, A.K., Broshek, D.K., Solomon, G.S., 2017. Predictors of clinical recovery from concussion: a systematic review. *Br. J. Sports Med.* 51, 941–948.
- Johnson, B., Zhang, K., Gay, M., Horovitz, S., Hallett, M., Sebastianelli, W., Slobounov, S., 2012. Alteration of brain default network in subacute phase of injury in concussed individuals: resting-state fMRI study. *NeuroImage* 59, 511–518.
- Kelly, A.C., Uddin, L.Q., Biswal, B.B., Castellanos, F.X., Milham, M.P., 2008. Competition between functional brain networks mediates behavioral variability. *NeuroImage* 39, 527–537.
- Krishnan, A., Williams, L., McIntosh, A., Abdi, H., 2011. Partial Least Squares (PLS) methods for neuroimaging: a tutorial and review. *NeuroImage* 56, 455–475.
- Li, W., Qin, W., Liu, H., Fan, L., Wang, J., Jiang, T., Yu, C., 2013. Subregions of the human superior frontal gyrus and their connections. *NeuroImage* 78, 46–58.
- Makkidssi, M., Darby, D., Maruff, P., Ugoni, A., Brukner, P., McCrory, P.R., 2010. Natural history of concussion in sport. *Am. J. Sports Med.* 38, 464–471.
- Makkidssi, M., Davis, G., Jordan, B., Patricios, J., Purcell, L., Putukian, M., 2013. Revisiting the modifiers: how should the evaluation and management of acute concussions differ in specific groups? *Br. J. Sports Med.* 47, 314–320.
- Mayer, A.R., Mannell, M.V., Ling, J., Gasparovic, C., Yeo, R.A., 2011. Functional connectivity in mild traumatic brain injury. *Hum. Brain Mapp.* 32, 1825–1835.
- McCrory, M., Kelly, J., Kluge, J., Ackley, B., Randolph, C., 1997. Standardized assessment of concussion in football players. *Neurology* 48, 586–588.
- McCrory, M., Guskiewicz, K., Marshall, S., Barr, W., Randolph, C., Cantu, R., Kelly, J., 2003. Acute effects and recovery time following concussion in collegiate football players: the NCAA Concussion Study. *JAMA* 290, 2556–2563.
- McCrory, P., Meeuwisse, W., Aubry, M., Cantu, B., Dvořák, J., Echemendia, R., Sills, A., 2013. Consensus statement on concussion in sport: the 4th International Conference on Concussion in Sport held in Zurich, November 2012. *Br. J. Sports Med.* 47, 250–258.
- Menon, V., Uddin, L.Q., 2010. Saliency, switching, attention and control: a network model of insula function. *Brain Struct. Funct.* 214, 655–667.
- Messé, A., Caplain, S., Pélégrini-Issac, M., Blanchon, S., Lévy, R., Aghakhani, N., Montreuil, M., Benali, H., Lehericy, S., 2013. Specific and evolving resting-state network alterations in post-concussion syndrome following mild traumatic brain injury. *PLoS One* 8, e65470.
- Mummary, C.J., Patterson, K., Price, C., Ashburner, J., Frackowiak, R., Hodges, J.R., 2000. A voxel-based morphometry study of semantic dementia: relationship between temporal lobe atrophy and semantic memory. *Ann. Neurol.* 47, 36–45.
- Pearlson, G.D., 1997. Superior temporal gyrus and planum temporale in schizophrenia: a selective review. *Prog. Neuro-Psychopharmacol. Biol. Psychiatry* 21, 1203–1229.
- Putukian, M., Echemendia, R., Dettwiler-Danspeckgruber, A., Duliba, T., Bruce, J., Furtado, J.L., Murugavel, M., 2015. Prospective clinical assessment using Sideline Concussion Assessment Tool-2 testing in the evaluation of sport-related concussion in college athletes. *Clin. J. Sport Med.* 25, 36–42.
- Rosipal, R., Krämer, N., 2006. Overview and recent advances in partial least squares. In: *Subspace, Latent Structure and Feature Selection.* Springer, Berlin Heidelberg, pp. 34–51.
- Sala-Llonch, R., Pena-Gomez, C., Arenaza-Urquijo, E.M., Vidal-Piñero, D., Bargallo, N., Junque, C., Bartres-Faz, D., 2012. Brain connectivity during resting state and subsequent working memory task predicts behavioural performance. *Cortex* 48, 1187–1196.
- Schweizer, T.A., Alexander, M.P., Cusimano, M., Stuss, D.T., 2007. Fast and efficient visuotemporal attention requires the cerebellum. *Neuropsychologia* 45, 3068–3074.
- Schweizer, T.A., Levine, B., Rewilak, D., O'Connor, C., Turner, G., Alexander, M.P., Cusimano, M., Manly, T., Robertson, I.H., Stuss, D.T., 2008. Rehabilitation of executive functioning after focal damage to the cerebellum. *Neurorehabil. Neural Repair* 22, 72–77.
- Shenton, M.E., Dickey, C.C., Frumin, M., McCarley, R.W., 2001. A review of MRI findings in schizophrenia. *Schizophr. Res.* 49, 1–52.
- Slobounov, S., Gay, M., Johnson, B., Zhang, K., 2012. Concussion in athletics: ongoing clinical and brain imaging research controversies. *Brain Imaging Behav.* 6, 224–243.
- Squire, L.R., Zola-Morgan, S., 1991. The medial temporal lobe memory system. *Science* 253, 1380.
- Strick, P.L., Dum, R.P., Fiez, J.A., 2009. Cerebellum and nonmotor function. *Annu. Rev. Neurosci.* 32, 413–434.
- Van Den Heuvel, M.P., Pol, H.E.H., 2010. Exploring the brain network: a review on resting-state fMRI functional connectivity. *Eur. Neuropsychopharmacol.* 20, 519–534.
- Viano, D.C., Casson, I.R., Pellman, E.J., Zhang, L., King, A.I., Yang, K.H., 2005. Concussion in professional football: brain responses by finite element analysis: part 9. *Neurosurgery* 57, 891–916.
- Vogt, B.A., 2016. Midcingulate cortex: structure, connections, homologies, functions and diseases. *J. Chem. Neuroanat.* 74, 28–46.
- Wong, C.W., Olafsson, V., Tal, O., Liu, T.T., 2012. Anti-correlated networks, global signal regression, and the effects of caffeine in resting-state functional MRI. *NeuroImage* 63, 356–364.
- Yuh, E.L., Hawryluk, G.W., Manley, G.T., 2014. Imaging concussion: a review. *Neurosurgery* 75, S50–S63.
- Zhang, K., Johnson, B., Pennell, D., Ray, W., Sebastianelli, W., Slobounov, S., 2010. Are functional deficits in concussed individuals consistent with white matter structural alterations: combined FMRI & DTI study. *Exp. Brain Res.* 204, 57–70.
- Zhou, Y., Milham, M.P., Lui, Y.W., Miles, L., Reaume, J., Sodickson, D.K., Grossman, R.I., Ge, Y., 2012. Default-mode network disruption in mild traumatic brain injury. *Radiology* 265, 882–892.
- Zhu, D., Covassin, T., Nogle, S., Doyle, S., Russell, D., Pearson, R., Kaufman, D., 2015. A potential biomarker in sports-related concussion: brain functional connectivity alteration of the default-mode network measured with longitudinal resting-state fMRI over thirty days. *J. Neurotrauma* 32, 327–341.